Adaptation of Limit-Cycle Walkers for Collaborative Tasks: A Supervisory Switching Control Approach

Sushant Veer, Mohamad Shafiee Motahar, and Ioannis Poulakakis

***Abstract*— This paper presents a method to achieve online gait adaptation of a dynamically walking biped when collaborating with an external agent—either a human or a robot—acting as a leader. Adaptation occurs without any explicit information on the leader's intended motion; only implicit information is used through the interaction force developed between the leader and the biped. An adaptive supervisory control scheme is proposed and guarantees for boundedness of the state despite switching under external force are provided. The supervisory controller leverages the availability of a library of exponentially stable limit-cycle gaits, and orchestrates switching among them in an online fashion to achieve adaptation. As a result, the range of leader speeds that the biped can adapt to is drastically enlarged while the leader's effort is reduced.**

I. Introduction

Robots often operate under uncertainty. This may arise due to intrinsic modeling errors or due to unknown or partially known interactions with the environment. An example of the latter occurs in the case where a robot physically collaborates with an external agent—another robot or a human—without explicit information regarding the collaborator's intentions. While a single controller provides the ability to handle only a certain amount of uncertainty, combining multiple controllers designed for different ranges of uncertain parameters can enlarge the span of influence of the augmented control strategy, and robustness could greatly be enhanced. This paper proposes an adaptive supervisory control scheme that switches among different controllers to enable adaptive dynamic locomotion of a biped collaborating with a leader moving at an unknown speed.

Collaborative tasks between bipedal robots—particularly, humanoids—and other robots or humans have been accomplished by adopting the Zero Moment Point (ZMP) criterion of stability; the book [1] provides an overview of such systems. Limit-cycle bipedal walkers, on the other hand, have not enjoyed the success of ZMP walkers in performing such tasks. So far, research efforts in these robots have been primarily focused on generating stable and robust gaits; see [2]–[4] for example. To enhance the robustness of limit-cycle walking gaits, a variety of methods have been proposed; these include the use of control Lyapunov functions [5], [6], event-based updates of virtual constraint parameters [7], and capture point methods for push recovery [8]. To engage limit-cycle walkers in tasks that involve their arms, dynamic locomotion controllers have been extended to incorporate manipulation in fully actuated bipeds in [9]. In this case, the controller is designed so that the walking gait remains unaffected by the manipulation task. In the context of dynamic bipeds collaborating with a leader, gait adaptation in response to interaction forces has been explored in the authors' previous work in [10], [11] and more recent work in [12]. However, the aforementioned efforts focus on a single limit cycle and do not exploit the availability of multiple such gaits.

The advantages of switching among multiple limit cycles to expand the capabilities of dynamically walking bipeds have been well recognized. Switching within a continuum of limit cycles was used in [13], [14] to perform speed change of such bipeds. To enhance robustness on rough terrain, [15] used a stochastic approach to switch between multiple controllers that stabilize dynamic gaits. A method for expanding the basin-of-attraction of a desired goal region in the state space by switching among stable limit cycles was presented in [16]. Similarly, [17] used Lyapunov estimates of the basin-of-attraction of stable limit-cycle gait primitives to achieve switching between them for the purposes of navigation of 3D bipeds amidst obstacles. In this paper, however, we shift the focus to the implications of switching for online gait adaptation in response to a leader.

This paper realizes online gait adaptation of an underactuated bipedal robot model to unknown desired trajectories of a leading collaborator. To achieve this, switching within a finite bank of HZD-based limit cycles is orchestrated by an adaptive supervisory controller [18, Chapter 6]. Leveraging the analytical nature of HZD, we present guarantees of stability while switching under the influence of external forces. Compared to our previous work [10], [11], the method in this paper provides a larger range of leader speeds that the biped can adapt to, while simultaneously reduces the effort required by the leader.

II. Overview: Adaptation for Cooperation

We are interested in collaborative tasks between a limit-cycle robotic walker and an external agent—either a robot or a human—that acts as the leader of the team. The leader's planned motion is represented as a trajectory $p_{\mathrm{L}}(t)$ which the robot is *unaware* of. Intuitively, the leader would apply an interaction force consistent with the desired motion $p_{\mathrm{L}}(t)$; for instance, the leader would pull the robot if walking faster is desirable. We will assume that this interaction force is available to the robot and use it as a cue to adapt the robot's speed to that of the leader. It was shown in previous work

S. Veer, M. S. Motahar and I. Poulakakis are with the Department of Mechanical Engineering, University of Delaware, Newark, DE 19716, USA; e-mail: {veer, motahar, poulakas}@udel.edu.

This work is supported in part by NSF CAREER Award IIS-1350721 and by NRI-1327614.

in [10] that the biped can adapt naturally in response to an external force. However, the range of leader speeds that can be accommodated is limited to the vicinity of the nominal unforced speed of the biped. This limitation is illustrated in Fig. 1 where a controller β_p designed for a nominal speed v_p can handle only a limited range of leader speeds v_{L}, represented as a colored ball.

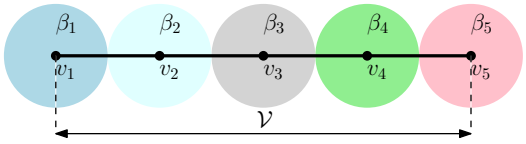

Fig. 1. Illustration of finite controllers spanning a set $\mathcal{V}$ within which an uncertain parameter takes values. The controller β_p is designed for a nominal value $v_p \in \mathcal{V}$ and it works when the true value v_{L} is in the vicinity of v_p, as illustrated by the colored balls.

One way to alleviate this issue is to generate multiple limit cycles corresponding to different nominal speeds $v_1, v_2, ...$ of the biped and switch among them in a suitable fashion, effectively enlarging the range of leader speeds that the biped can adapt to, while reducing the effort required by the leader. The controllers that generate these nominal motions are indexed by $\beta_1, \beta_2, ...$, and they are archived in a bank of controllers as shown in Fig. 2. The biped must now make decisions as to which controller should be placed in the loop to facilitate adaptation to the leader's unknown intended motion $p_{\mathrm{L}}(t)$. To achieve this objective, this paper proposes the adaptive supervisory controller depicted in Fig. 2.

The proposed control architecture is organized on two levels, as shown in Fig. 2. On the low level, a family of hybrid control laws, suitably parametrized by a parameter array β, is designed based on feedback from the state and the external force. On the high level, the supervisor decides which controller will be used over the next step based on online measurements of the robot's state. These measurements form a monitoring signal μ, which effectively assigns a "cost" to each of the candidate controllers in the controller bank. The monitoring signal is then processed by the switching logic, which outputs a switching signal $\sigma(k)$ that evaluates the index p of the controller β_p with the least cost. This controller is the one that is placed in the loop over the next step. The following sections provide details

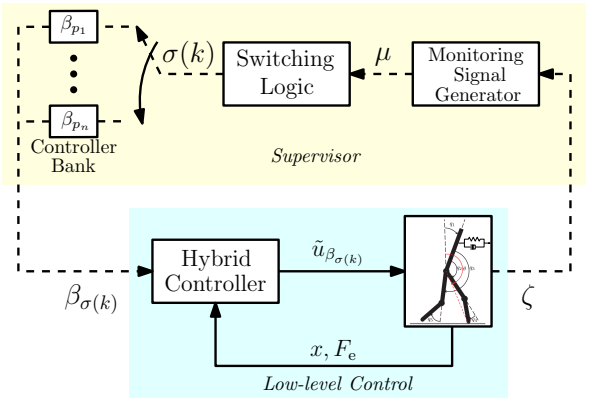

Fig. 2. Supervisory control block diagram. The high-level supervisor is shown in yellow and the low-level execution loop is shown in blue. Signals flow along the solid channels during the continuous-time (swing phase) and along the dashed during the discrete phase (instantaneous double support).

regarding the design of the components that compose the proposed adaptive supervisory controller.

III. Modeling a Planar Bipedal Walker

We consider a fairly generic model of a bipedal robot walking under the influence of an external agent, whose intention is experienced by the biped through an interaction force, as shown in Fig. 3. The model corresponds to the geometry and parameters of the bipedal robot RABBIT [4].

To simulate the interaction force, we employ an impedance model that translates the leader's intended trajectory $p_{\mathrm{L}}(t)$ to a force $F_{\mathrm{e}}(t)$ applied on the robot model at point E, as shown in Fig. 3. Mathematically,

$$F_{\mathrm{e}} = K_{\mathrm{L}}(p_{\mathrm{L}} - p_{\mathrm{E}}) + N_{\mathrm{L}}(\dot{p}_{\mathrm{L}} - \dot{p}_{\mathrm{E}}) \ , \tag{1}$$

where K_{L}, N_{L} are impedance gains and p_{E} is the position of the point E. Further details on the interaction model can be found in [11, Section II.A]; we will only mention here that F_{e} is assumed to be a smooth and bounded function of time as in [10, Section II].

The model of the biped has five degrees of freedom (DoF). Four actuated DoFs correspond to the hip and knee joints of the two legs, and one unactuated DoF to the pivot joint representing the contact between the toe of the support leg and the ground, thus resulting in one degree of underactuation. The generalized coordinates of the robot q are chosen as shown in Fig. 3, and take values in some suitable set Q. Let $x := (q^{\mathrm{T}}, \dot{q}^{\mathrm{T}})^{\mathrm{T}} \in TQ$ denote the system's state. Walking is modeled as an alternating sequence of swing and instantaneous double support phases, resulting in the following system with impulse effects

$$\Sigma: \begin{cases} \dot{x} = f(x) + g(x)u + g_{\mathrm{e}}(x)F_{\mathrm{e}}, & x \in TQ \setminus \mathcal{S} \\ x^+ = \Delta(x^-), & x^- \in \mathcal{S}. \end{cases} \tag{2}$$

In this model, f, g and g_{e} are vector fields describing the continuous-time dynamics during the swing phase under the influence of the control inputs u and the externally applied force F_{e}. The continuous-time evolution of the swing dynamics is interrupted when the swing leg touches the ground surface, defined as

$$\mathcal{S} := \{(q, \dot{q}) \in TQ \mid p_{\mathrm{v}}(q) = 0, \ \dot{p}_{\mathrm{v}}(q, \dot{q}) < 0\} \ , \tag{3}$$

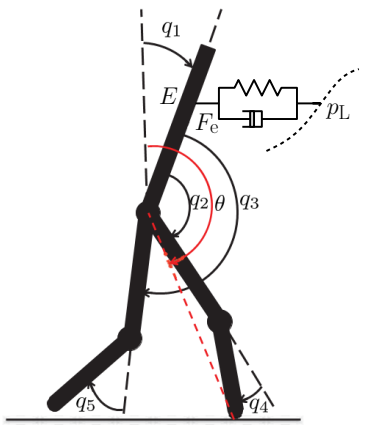

Fig. 3. Robot model with a choice of generalized coordinates.

where $p_{\rm v}(q)$ is the height of the swing foot. Assuming that the subsequent double support phase is instantaneous as in [4], the state undergoes a discontinuous jump according to the map $\Delta : \mathcal{S} \to TQ$, that captures the physics of the impact, and takes the pre-impact state $x^- \in \mathcal{S}$ to a post-impact state $x^+ \in TQ$.

IV. Low-Level Control Design

We now proceed with designing a family of feedback control laws for (2). As we will see, these control laws will be indexed by a parameter array β, which corresponds to different walking motions in the biped of Fig. 3. Consider a set of outputs of the form

$$y_\beta = h_\beta(q) = q_{\rm a} - h_{\rm d}(\theta) - h_{\rm s}(\theta, \beta) \tag{4}$$

associated with the continuous-time dynamics of (2). Here, $q_{\rm a}$ includes the actuated DoFs, i.e., $q_{\rm a} := (q_2, q_3, q_4, q_5)$, and $h_{\rm d}(\theta) + h_{\rm s}(\theta, \beta)$ is their desired evolution, represented as a function of the angle $\theta(q) := q_1 + q_2 + \frac{1}{2}q_4$ shown in Fig. 3. Note that the term $h_{\rm s}(\theta, \beta)$ is a polynomial of θ with coefficients that depend on the parameter array β, and it will be designed below.

The objective of the control input u in (2) is to drive the output (4) to zero, and it can be achieved by differentiating (4) with respect to time to obtain the input/output relationship

$$\ddot{y}_\beta = L_f^2 h_\beta(x) + L_g L_f h_\beta(x) u + L_{g_{\rm e}} L_f h_\beta(x) F_{\rm e} \ . \tag{5}$$

Assuming that the force $F_{\rm e}$ can be measured and that the decoupling matrix $L_g L_f h_\beta(x)$ is invertible, the control law

$$u^*_\beta(x, F_{\rm e}) = -L_g L_f h_\beta(x)^{-1} [L_f^2 h_\beta(x) + L_{g_{\rm e}} L_f h_\beta(x) F_{\rm e}] \tag{6}$$

renders the zero dynamics surface

$$\mathcal{Z}_\beta := \{(q, \dot{q}) \in TQ \mid h_\beta(q) = 0, \ L_f h_\beta(q, \dot{q}) = 0\} \tag{7}$$

invariant under the swing dynamics of (2).

Next, we require that the surface $\mathcal{Z}_\beta$ is invariant under the impact map Δ; that is, $\mathcal{Z}_\beta$ is hybrid invariant. This property can be achieved by properly designing the polynomials $h_{\rm d}$ and $h_{\rm s}$. In more detail, we begin by requiring

$$h_{\rm s}(\theta, 0) \equiv 0 \ , \tag{8}$$

i.e., $h_{\rm s}$ vanishes identically when $\beta = 0$. We can then design $h_{\rm d}$ as in [4, Section 6.2] to achieve hybrid invariance of the zero dynamics surface $\mathcal{Z}$ corresponding to $\beta = 0$; note that, as established in [10, Section II], the presence of $F_{\rm e}$ does not "break" hybrid invariance of $\mathcal{Z}$. The final step is to extend hybrid invariance to the surfaces $\mathcal{Z}_\beta$ for non-zero values of β. This can be achieved by imposing the conditions

$$\begin{cases} h_{\rm s}(\theta^+, \beta) = 0, \ \dfrac{\partial h_{\rm s}}{\partial \theta}(\theta^+, \beta) = 0 \\ h_{\rm s}(\theta_s, \beta) = 0, \ \dfrac{\partial^i h_{\rm s}}{\partial \theta^i}(\theta_s, \beta) = 0, \ i = 1, 2 \\ h_{\rm s}(\theta, \beta) = 0, \quad \text{for} \quad \theta_s \le \theta \le \theta^- \end{cases} \tag{9}$$

where θ^+ and θ^- denote the post- and pre-impact values of θ in the course of a step, and $\theta_{\rm s} = \theta^+ + 0.9(\theta^- - \theta^+)$. Essentially, the polynomials $h_{\rm s}(\theta, \beta)$ vanish at the post-impact instant (when $\theta = \theta^+$) and after 90% of the step is completed (when $\theta \in [\theta_{\rm s}, \theta^-)$). As a result of (9), hybrid invariance of $\mathcal{Z}_\beta$ can be established provided that $\mathcal{Z}$ is hybrid invariant; see [14, Lemma 1]. Intuitively, the "deformation" introduced on the surface $\mathcal{Z}$ due to non-zero values of β is such that the resulting surfaces $\mathcal{Z}_\beta$ are smoothly connected back to $\mathcal{Z}$ towards the end of the step. An important consequence of designing $h_{\rm s}(\theta, \beta)$ to satisfy (9) is that $\mathcal{S} \cap \mathcal{Z}_\beta = \mathcal{S} \cap \mathcal{Z}$, which is a one-dimensional surface in TQ. This property greatly facilitates switching among multiple controllers, as will be discussed in Section V.

The aforementioned geometric constructions lead to the emergence of a well defined *Forced Hybrid Zero Dynamics (FHZD)*, which was introduced in [10] to capture the effect of the external force on the motion of the system. Consider (2) in closed loop with the control law u^*_β of (6) and let $z := (\theta, \zeta)$ be a set of coordinates on the surfaces $\mathcal{Z}_\beta$. As shown in [10, Lemma 1], we have $\zeta := \frac{1}{2}(D_1(q)\dot{q})^2$ where $D_1(q)$ is the first row of the robot's inertia matrix $D(q)$ corresponding to q_1. Intuitively, ζ represents a measure of the kinetic energy of the system while evolving on $\mathcal{Z}$. Using the hybrid invariance of $\mathcal{Z}_\beta$ under the dynamics of (2) and the property $\mathcal{S} \cap \mathcal{Z}_\beta = \mathcal{S} \cap \mathcal{Z}$, the reduced-order forced Poincaré map $\rho_\beta : (\mathcal{S} \cap \mathcal{Z}) \times \mathbb{R} \to (\mathcal{S} \cap \mathcal{Z})$ can be computed explicitly as in [10] to result in

$$\rho_\beta(\zeta, w) = \delta_{\rm z}^2 \zeta - v_\beta + w \ , \tag{10}$$

where $0 < \delta_{\rm z} < 1$ and v_β are constants, while w is a forcing term, the value of which can vary from one step to the next depending on the external force $F_{\rm e}$. Intuitively, w represents the "work" done by $F_{\rm e}$ on the solution of the closed-loop system as it evolves along $\mathcal{Z}_\beta$. Notice that $\delta_{\rm z}$ is independent of β, which is an outcome of (9); see [14, Theorem 1]. The expressions of v_β and w can be found in [10, Section III] and are omitted here for the sake of brevity.

The reduced-order forced Poincaré map (10) gives rise to a discrete-time dynamical system, namely, the FHZD,

$$\zeta[k+1] = \rho_\beta(\zeta[k], w[k]) \ , \tag{11}$$

with an unforced ($w \equiv 0$) fixed point

$$\zeta^*_\beta = -\frac{v_\beta}{1 - \delta_{\rm z}^2} \ , \tag{12}$$

corresponding to a periodic walking gait, which is exponentially stable due to the fact that $0 < \delta_{\rm z} < 1$. As β varies, a continuum of such motions can be generated. It is emphasized that (11) is a one-dimensional system; as we will see in Section V below, this dimensional reduction will greatly facilitate switching among different controllers, as required by the supervisory controller of Fig. 2. Finally, note that by [19, Lemma 1], the fixed point ζ^*_β of (11) is locally input-to-state stable (ISS) with respect to the forcing term w, provided that[1] w remains within a bounded set. This

[1]Note that even though the main ISS result in [19] is presented for a class of piecewise constant forces, the ISS property on the zero dynamics [19, Lemma 1] holds for piecewise smooth forces.

ensures that the biped can continue taking steps for forces with sufficiently small magnitude, implying that the FHZD of (11) is well defined.

V. Adaptive Supervisory Control Design

This section provides details regarding the components of the supervisory controller depicted in Fig. 2. The purpose of this controller is to orchestrate switching among low-level control laws in order to realize adaptable locomotion.

A. Switching Among a Finite Bank of Controllers

Out of the continuum of unforced exponentially stable fixed points ζ^*_β that are available by varying β, we extract a finite subcollection $\zeta^*_{\beta_p}$, indexed by $p \in \mathcal{P}$, where $\mathcal{P}$ is a finite index set. In the case of speed adaptation, these fixed points correspond to limit-cycle walking motions with different forward speeds. The control parameters β_p index the corresponding control laws $u^*_{\beta_p}$, which are assembled in a bank of controllers $\mathbb{B} := \{\beta_p, p \in \mathcal{P}\}$, as shown in Fig. 2. Given $\mathbb{B}$, it is important to be able to state conditions under which the dynamics induced by switching among the controllers in $\mathbb{B}$ on the basis of the external force will not cause instability. To address this issue, we develop a switched system with multiple equilibria.

Let $\sigma : \mathbb{Z}_+ \to \mathcal{P}$ be a switching signal, which maps the step number $k \in \mathbb{Z}_+$ to the index $p = \sigma(k)$ that corresponds to the controller $u^*_{\beta_p}$ of (6) that is placed in the loop. The signal σ is generated by the switching logic that will be discussed below in Section V-B. To simplify notation, from hereon we will denote the index β_p simply by p. Based on the discussion in Section IV, the geometric structure introduced by the control laws ensures that $\mathcal{S} \cap \mathcal{Z}_p = \mathcal{S} \cap \mathcal{Z}$ for all $p \in \mathcal{P}$. Hence, despite the presence of the external force, as long as $z[0] \in \mathcal{S} \cap \mathcal{Z}_{\sigma(0)}$, the discrete evolution of the system always occurs on the one dimensional surface $\mathcal{S} \cap \mathcal{Z}$ and can be captured by the switched system

$$\zeta[k+1] = \rho_{\sigma(k)}(\zeta[k], w[k]) \ , \tag{13}$$

which effectively captures switching among the reduced systems (11). Hence, the dimensional reduction associated with an individual FHZD controller is retained despite switching among multiple controllers, provided that the initial conditions do not excite dynamics transversal to the surfaces $\mathcal{Z}_p$. This fact facilitates the study of the behavior of the system under switching among multiple controllers. Note though that the mappings ρ_p, $p \in \mathcal{P}$ in (13) do not share a common equilibrium point as in the classical switched systems theory [18].

Due to the one-dimensional nature of (13) we can provide explicit conditions, under which the dynamics induced by switching among controllers in $\mathbb{B}$ do not result in the biped falling. Consider the fixed points ζ^*_p, $p \in \mathcal{P}$, and let $\zeta^*_{\rm lb} := \min_{p\in\mathcal{P}} \zeta^*_p$, and $\zeta^*_{\rm ub} := \max_{p\in\mathcal{P}} \zeta^*_p$. We can then prove the following result that guarantees that the state ζ of the switching system (13) will remain bounded under switching.

Theorem 1 (Switching Under External Force): Consider (13). Suppose that $w_{\rm lb} \in \mathbb{R}$ and $w_{\rm ub} \in \mathbb{R}$ are such that $w_{\rm lb} \le w[k] \le w_{\rm ub}$ for all $k \in \mathbb{Z}_+$ and for all $p \in \mathcal{P}$, the reduced maps ρ_p are well-defined on the domain

$$\mathcal{D} := \big[\zeta^*_{\rm lb} + \frac{w_{\rm lb}}{1-\delta_{\rm z}^2},\ \zeta^*_{\rm ub} + \frac{w_{\rm ub}}{1-\delta_{\rm z}^2}\big] \ . \tag{14}$$

Then, for any switching signal $\sigma(k)$, we have that

$$\zeta[0] \in \mathcal{D} \ \Rightarrow \ \zeta[k] \in \mathcal{D} \tag{15}$$

for all steps $k \in \mathbb{Z}_+$.

The proof of Theorem 1 is given in the Appendix. Intuitively, this result guarantees that under external forces with sufficiently small magnitude so that $w \in [w_{\rm lb},\ w_{\rm ub}]$, the state of the biped remains bounded under arbitrary switches, thereby ensuring that the biped will keep taking well-defined steps.

B. Monitoring Signal Generator and Switching Logic

Having established conditions under which switching in the presence of the external force does not result in failure to walk, we now turn our attention to determining the logic that orchestrates switching so that the biped can adapt its speed to the (unknown) speed of the external collaborator.

As mentioned in Section II, the objective of the monitoring signal generator is to assign a "cost" to each controller $u^*_{\beta_p}$ in $\mathbb{B}$, which reflects how suitable this controller is given the state ζ of the system. A natural choice is to consider the error between the current value of the state $\zeta[k]$ and the fixed point ζ^*_p; i.e.,

$$\mu_p(k) := |\zeta[k] - \zeta^*_p| \ . \tag{16}$$

This choice dictates that the cost associated with a controller $u^*_{\beta_p}$ is low when the corresponding fixed point ζ^*_p is close to the current value of the state ζ. Note that μ_p is the instantaneous value of the error at the k-th step; other choices for constructing monitoring signals, that take into account their past behavior can be found in [18].

With μ_p available for all $p \in \mathcal{P}$, a reasonable choice for the switching logic is to place in the loop the controller β_p whose index p corresponds to the monitoring signal μ_p that is currently the smallest; i.e.,

$$\sigma(k) = \arg\min_{p\in\mathcal{P}} \mu_p(k) \ . \tag{17}$$

In words, the underlying switching strategy consists of selecting, at each step, the candidate controller known to stabilize the fixed point ζ^*_p, the monitoring signal μ_p of which is currently the smallest. It should be emphasized that, in general, arbitrary switching among exponentially stable equilibria may lead to divergence of the state [18]. However, under the conditions stated in Theorem 1, this does not raise any concern and switching can occur arbitrarily frequently, at the end of any step.

VI. Speed Adaptation to a Leader

We consider the scenario briefly described in Section II. Without loss of generality, we will restrict our attention to the case in which the leader walks with an *unknown* constant speed $v_{\rm L}$ taking values in a compact set $\mathcal{V}$; that is, $\dot{p}_{\rm L} = v_{\rm L} \in \mathcal{V}$. The set $\mathcal{V}$ represents the uncertainty region.

A. Implementation Aspects

For practical implementation, the low-level controllers of Section IV must be able to handle perturbations away from $\mathcal{Z}_\beta$ while respecting actuator saturation constraints as well as friction cone limitations. To achieve these additional objectives, the control law (6) is augmented with an auxiliary control variable $\nu(y_\beta, \dot{y}_\beta)$, which will be designed here using a Control Lyapunov Function (CLF) combined with a Quadratic Program (QP) as in [20]. However, the constraints added in the QP to accommodate actuator saturation and friction limitations may violate the hybrid invariance of $\mathcal{Z}_\beta$ and affect the transient response. We have found that modifying the output h_β in (4) as in

$$\tilde{y}_\beta = \tilde{h}_\beta(q, y_{\rm i}, \dot{y}_{\rm i}) := q_{\rm a} - h_{\rm d}(\theta) - h_{\rm s}(\theta, \beta) - h_{\rm c}(\theta, y_{\rm i}, \dot{y}_{\rm i}) \quad (18)$$

improves transient behavior. In (18), the term $h_{\rm c}(\theta, y_{\rm i}, \dot{y}_{\rm i})$ is a correction polynomial, the coefficients of which depend on $y_{\rm i} = h_\beta(q^+)$ and $\dot{y}_{\rm i} = L_f h_\beta(q^+, \dot{q}^+)$. More details on the design of $h_{\rm c}$ can be found in [21]; we only mention here that $h_{\rm c}(\theta, y_{\rm i}, \dot{y}_{\rm i})$ is such that it vanishes by the end of the step and $h_{\rm c}(\theta, 0, 0) \equiv 0$. With this modification, the low-level controller takes the form

$$\tilde{u}_\beta = -L_g L_f \tilde{h}_\beta^{-1} [L_f^2 \tilde{h}_\beta + L_{g_{\rm e}} L_f \tilde{h}_\beta F_{\rm e} + \nu] \ , \qquad (19)$$

where ν is generated using a CLF-QP as in [20]. It is remarked that using the modified output $\tilde{h}_\beta$ instead of h_β in the low-level controller (19) is not necessary; however, in the simulations below we adopt (19) as it results in better transient behavior.

With the control law (19) available, we can extract the subcollection $\mathbb{B}$ used by the supervisor. The finite elements in $\mathbb{B}$ must be selected so that the limit cycles $\zeta^*_{\beta_p}$, $\beta_p \in \mathbb{B}$ correspond to forward speeds that sufficiently "cover" the uncertainty region $\mathcal{V}$. The fact that a finite collection of controllers in $\mathbb{B}$ can cover the uncountably infinite uncertainty set $\mathcal{V}$ is a consequence of the natural adaptation of the closed-loop biped to the leader's speed. Indeed, as was shown in [10], [11], when the leader's speed $v_{\rm L}$ is sufficiently close to the speed of an unforced limit cycle $\zeta^*_{\beta_p}$, the biped accelerates or decelerates depending on the externally applied force so that it matches the leader's speed. Hence, there is a range of leader speeds—illustrated as an open ball in Fig. 1—that can be accommodated by a single controller, even when switching among different controllers is not present. Hence, to construct $\mathbb{B}$, we select a finite set of limit cycles, each having the property to adapt to a range of leader's speeds so that the union of these ranges covers the entire $\mathcal{V}$.

B. Evaluation in Simulation

The speed of the leader $v_{\rm L}$ is allowed to be any number in the uncertainty set $\mathcal{V} := [0.45, 0.81]$ m/s, and the impedance parameters in (1) are chosen as $K_{\rm L} = 15$ N/m, $N_{\rm L} = 10$ Ns/m. For the simulations below, the motor saturation torque is assumed to be 100 Nm. The coefficient of friction with the ground is taken equal to 0.8 and a minimum upwards vertical force of 100 N at the stance foot is imposed to ensure that no sliding occurs. These constraints are incorporated in the QP associated with the controller design. Using the method described in Section IV, by picking different β_p we generate 79 exponentially stable limit cycles with unforced nominal speeds varying from 0.42 m/s to 0.81 m/s. The controllers for these limit cycles were indexed in an ascending order of speed to form the controller bank $\mathbb{B}$.

In the examples shown in Figs. 4 and 5 the leader's intended speed is $v_{\rm L} = 0.81$ m/s, and is unknown to the biped. Without the adaptive supervisory controller, if the biped starts at any limit cycle with an average speed below 0.65 m/s, the controller is unable to comply with the saturation torque and friction limitations imposed, resulting in failure to adapt to the leader's motion. However, as shown in Fig. 4(a), with the supervisor switching among different controllers, successful convergence of the biped to the leader's intended speed is observed, even when the biped initially walks at 0.45 m/s. It is seen in Fig. 4(b) that the biped switches its limit cycle to bring its nominal unforced speed in close proximity to the leader's intended speed. The Root Mean Square (RMS) of the force applied by the leader is shown in Fig. 4(c). It is observed that the RMS of the force is high in the beginning but it reduces as the biped adapts to a limit cycle with nominal speed close to $v_{\rm L}$.

With the supervisor in the control loop, a marked improvement in the effort required by the leader was observed. This is demonstrated in Fig. 5 where the biped starts at a limit cycle with nominal speed of 0.65 m/s while the leader's intended speed is 0.81 m/s. The RMS of the force when no switching is permitted takes values above 10 N, while the RMS of the force with the supervisory controller in the loop takes values below 7 N. Hence, a substantial improvement is achieved through the introduction of the supervisor, both in terms of the range of speed that the biped can adapt to and the effort required by the leader.

VII. Conclusion

This paper presented a method to achieve online gait adaptation of dynamically walking bipedal robots under external force by switching among pre-computed limit cycles. The motivation behind this work is to achieve collaborative human-robot object transportation. The proposed method leverages the dimensional reduction and the analytical nature of HZD-based control design along with the flexibility afforded by adaptive supervisory control schemes to enable the biped to handle a broader range of leader speeds while reducing the effort required for adaptation. These results form a first step toward the development of a framework for adaptive switching among stable bipedal gaits to accommodate uncertain or unknown interactions with the environment.

Appendix

The proof of Theorem 1 is by induction on the step number k. The induction begins at $k = 0$ where it is given that $\zeta[0] \in \mathcal{D}$. To take the induction step, let $k \in \mathbb{Z}_+$ be arbitrary and assume $\zeta[k] \in \mathcal{D}$. We will show that $\zeta[k+1] \in \mathcal{D}$.

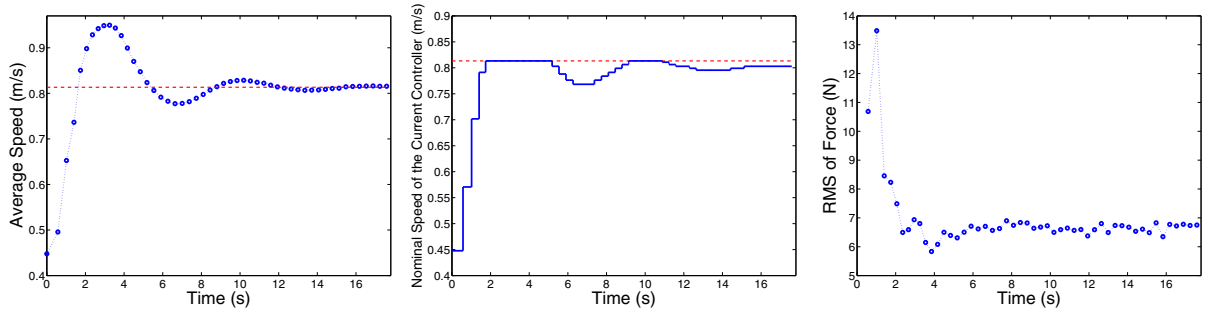

(a) (b) (c)

Fig. 4. Response of the biped when the leader's intended speed is faster than the biped's speed. (a) Dashed red line is the leader's intended speed $v_{\mathrm{L}} = 0.81$ m/s; blue marker is the step-wise average speed of the biped. (b) Dashed red line is the leader's intended speed $v_{\mathrm{L}} = 0.81$ m/s; blue line is the speed of the nominal orbit for the controller in loop. (c) RMS of the force applied by the leader over each step.

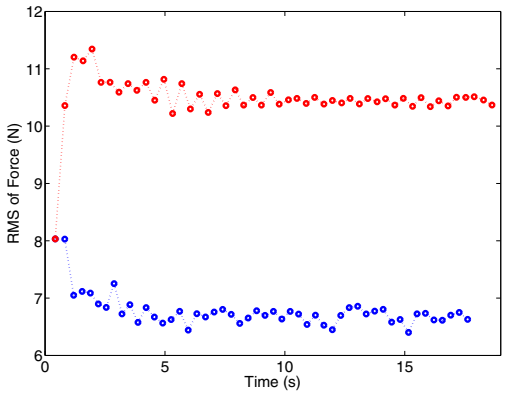

Fig. 5. Interaction force with (blue) and without (red) supervisory control.

Indeed, using (12) in (10) we have

$$\zeta[k+1] = \delta_{\mathrm{z}}^2 \zeta[k] + (1-\delta_{\mathrm{z}}^2)\zeta^*_{\sigma(k)} + w[k] \ . \qquad (20)$$

Noting that $1-\delta_{\mathrm{z}}^2 > 0$ and $\zeta^*_{\mathrm{lb}} \leq \zeta^*_{\sigma(k)} \leq \zeta^*_{\mathrm{ub}}$ it follows that

$$\begin{aligned} \delta_{\mathrm{z}}^2(\zeta[k]-\zeta^*_{\mathrm{lb}}) + \zeta^*_{\mathrm{lb}} + w_{\mathrm{lb}} &\leq \zeta[k+1] \qquad (21) \\ &\leq \delta_{\mathrm{z}}^2(\zeta[k]-\zeta^*_{\mathrm{ub}}) + \zeta^*_{\mathrm{ub}} + w_{\mathrm{ub}} \ . \end{aligned}$$

As $\zeta[k] \in \mathcal{D}$, we have $\zeta[k] - \zeta^*_{\mathrm{lb}} \geq \frac{w_{\mathrm{lb}}}{1-\delta_{\mathrm{z}}^2}$ and $\zeta[k] - \zeta^*_{\mathrm{ub}} \leq \frac{w_{\mathrm{ub}}}{1-\delta_{\mathrm{z}}^2}$. Using these in upper and lower bounds of (21) gives

$$\begin{aligned} \delta_{\mathrm{z}}^2(\zeta[k]-\zeta^*_{\mathrm{lb}}) + \zeta^*_{\mathrm{lb}} + w_{\mathrm{lb}} &\geq \zeta^*_{\mathrm{lb}} + \frac{w_{\mathrm{lb}}}{1-\delta_{\mathrm{z}}^2} \ , \\ \delta_{\mathrm{z}}^2(\zeta[k]-\zeta^*_{\mathrm{ub}}) + \zeta^*_{\mathrm{ub}} + w_{\mathrm{ub}} &\leq \zeta^*_{\mathrm{ub}} + \frac{w_{\mathrm{ub}}}{1-\delta_{\mathrm{z}}^2} \ . \end{aligned}$$

With the above inequalities and (21) we get $\zeta[k+1] \in \mathcal{D}$.

REFERENCES

[1] K. Harada, E. Yoshida, and K. Yokoi, Eds., *Motion Planning for Humanoid Robots*. Springer-Verlag, 2010.

[2] R. D. Gregg and M. W. Spong, "Reduction-based control of three-dimensional bipedal walking robots," *Int. J. of Robotics Research*, vol. 29, no. 6, pp. 680–702, May 2009.

[3] L. B. Freidovich, U. Mettin, A. S. Shiriaev, and M. W. Spong, "A passive 2-DOF walker: Hunting for gaits using virtual holonomic constraints," *IEEE Transactions on Robotics*, vol. 25, no. 5, pp. 1202–1208, October 2009.

[4] E. R. Westervelt, J. W. Grizzle, C. Chevallereau, J. H. Choi, and B. Morris, *Feedback Control of Dynamic Bipedal Robot Locomotion*. Boca Raton, FL: CRC Press, 2007.

[5] Q. Nguyen and K. Sreenath, "Optimal robust control for bipedal robots through control lyapunov function based quadratic programs," in *Proc. of Robotics: Science and Systems*, 2015.

[6] S. Kolathaya and A. D. Ames, "Parameter to state stability of Control Lyapunov Functions for hybrid system models of robots," *Nonlinear Analysis: Hybrid Systems*, 2016.

[7] K. A. Hamed and J. W. Grizzle, "Event-based stabilization of periodic orbits for underactuated 3-D bipedal robots with left-right symmetry," *IEEE Transactions on Robotics*, vol. 30, no. 2, pp. 365–381, 2014.

[8] J. Pratt, J. Carff, S. Drakunov, and A. Goswami, "Capture point: A step toward humanoid push recovery," in *Proc. of IEEE-RAS Int. Conf. on Humanoid Robots*, Genoa, December 2006, pp. 200–207.

[9] A. D. Ames and M. Powell, "Towards the unification of locomotion and manipulation through control lyapunov functions and quadratic programs," in *Control of Cyber-Physical Systems, Lecture Notes in Control and Information Sciences*. Springer, 2013, pp. 219–240.

[10] S. Veer, M. S. Motahar, and I. Poulakakis, "On the adaptation of dynamic walking to persistent external forcing using hybrid zero dynamics control," in *Proc. of IEEE/RSJ Int. Conf. on Intelligent Robots and Systems*, Hamburg, September 2015, pp. 997–1003.

[11] M. S. Motahar, S. Veer, J. Huang, and I. Poulakakis, "Integrating dynamic walking and arm impedance control for cooperative transportation," in *Proc. of IEEE/RSJ Int. Conf. on Intelligent Robots and Systems*, Hamburg, September 2015, pp. 1004–1010.

[12] M. S. Motahar, S. Veer, and I. Poulakakis, "Steering a 3D limit-cycle walker for collaboration with a leader," in *Proc. of IEEE/RSJ Int. Conf. on Intelligent Robots and Systems*, Vancouver, September 2017.

[13] X. Da, O. Harib, R. Hartley, B. Griffin, and J. Grizzle, "From 2D design of underactuated bipedal gaits to 3D implementation: Walking with speed tracking," *IEEE Access*, vol. 4, pp. 3469 – 3478, July 2016.

[14] S. Veer, M. S. Motahar, and I. Poulakakis, "Generation of and switching among limit-cycle bipedal walking gaits," in *Proc. of IEEE Conf. on Decision and Control*, Melbourne, December 2017.

[15] C. O. Saglam and K. Byl, "Robust policies via meshing for metastable rough terrain walking," in *Proc. of Robotics: Science and Systems*, 2014.

[16] R. Tedrake, I. R. Manchester, M. Tobenkin, and J. W. Roberts, "LQR-trees: Feedback motion planning via sums-of-squares verification," *Int. J. of Robotics Research*, vol. 29, no. 8, pp. 1038–1052, 2010.

[17] M. S. Motahar, S. Veer, and I. Poulakakis, "Composing limit cycles for motion planning of 3D bipedal walkers," in *Proc. of IEEE Conf. on Decision and Control*, Las Vegas, December 2016.

[18] D. Liberzon, *Switching in Systems and Control*. Birkhäuser, 2003.

[19] S. Veer, M. S. Motahar, and I. Poulakakis, "Local input-to-state stability of dynamic walking under persistent external excitation using hybrid zero dynamics," in *Proc. of the American Control Conf.*, Boston, July 2016, pp. 4801–4806.

[20] Q. Nguyen, X. Da, J. Grizzle, and K. Sreenath, "Dynamic walking on stepping stones with gait library and control barrier functions," in *Proc. of the Int. Workshop On the Algorithmic Foundations of Robotics*, San Francisco, December 2016.

[21] B. Morris and J. W. Grizzle, "Hybrid invariant manifolds in systems with impulse effects with application to periodic locomotion in bipedal robots," *IEEE Transactions on Automatic Control*, vol. 54, no. 8, pp. 1751–1764, August 2009.